IET Smart Grid

Research Article

IET Journals
The Institution of Engineering and Technology

Fuel cell integrated unified power quality conditioner for voltage and current reparation in four-wire distribution grid

eISSN 2515-2947
Received on 28th July 2018
Revised 10th October 2018
Accepted on 1st November 2018
E-First on 23rd January 2019
doi: 10.1049/iet-stg.2018.0148
www.ietdl.org

Chinnayan Karuppaiyah Sundarabalan[1] ✉, *Yeseswini Puttagunta*[1], *Vedhamoorthy Vignesh*[1]

[1]*EEE Department, SASTRA Deemed University, Thanjavur, Tamilnadu, India*

✉ *E-mail: ckseee@yahoo.com*

Abstract: Electrical and electronic devices, when exposed to one or more power quality problems, are prone to failure. This study aims to enhance the quality of power in three-phase four-wire distribution grid using fuel cell integrated unified power quality conditioner (FCI-UPQC). The proposed FCI-UPQC has a four-leg converter on the shunt side and three-leg converter on the series side. A combination of a synchronous reference frame and instantaneous reactive power theories is utilised to generate reference signals of the FCI-UPQC. Also, this study proposes an adaptive neuro-fuzzy inference system (ANFIS) controller to maintain the DC-link voltage in the FCI-UPQC. The ANFIS controller is designed like a Sugeno fuzzy architecture and trained offline using data from the proportional–integral controller. The obtained results proved that the proposed FCI-UPQC compensated power quality problems such as voltage sag, swell, harmonics, neutral current, source current imbalance in the three-phase four-wire distribution grid. The presence of fuel cell in this work makes more effectiveness of the proposed system by providing real power support during supply interruption on the grid side.

Nomenclature

R	gas constant, 8.3143 J/(mole, K)
F	Faraday constant, 96,487 (C/mole)
E_0°	standard reference potential at standard state, 298 K at 1 atm pressure
η	temperature invariant part of V_a in V
T	internal temperature
I_{FC}	fuel cell current
I_{lim}	limitation current (A)
Z	number of electrons
R_a	equivalent resistances of activation voltage drop
R_c	equivalent resistances of concentration voltage drop
R_o	ohmic resistance
E_o	reference potential which is a function of T
k_{RI}	empirical constant for calculating R_o, (r/A)
k_{RT}	empirical constant for calculating R_o, (r/K)
V_{FC}	fuel cell voltage
V_{sa}, V_{sb}, V_{sc}	source voltage
I_{La}, I_{Lb}, I_{Lc}	load current
I_a*, I_b*, I_c*	converter current
V_{L2a}, V_{L2b}, V_{L2c}	load voltage

1 Introduction

Power quality is the set of limits of electrical properties that allows the electrical system to function in a proper manner without significant loss [1]. Due to the latest inventions of power electronic devices like adjustable speed drives, switching of loads and so on lead to non-linearity in the supply [2]. Any deviation in current, voltage or frequency from the reference values leads to failure customer's equipment, loss of production and damage to equipment [3]. Hence, it is essential to retain high quality power.

In recent years, custom power devices (CPDs) become smarter in the distribution grid due to their effectiveness in the alleviation of power quality problems [2]. The unified power quality conditioner (UPQC) is one of the effective CPD and its topology consists of the integration of two active power filters connected in a back-to-back configuration to a common DC-link bus [4]. The UPQC combines both the operations of load current and supply voltage imperfections with quick response and high reliability at the same time [5–8]. The fuel cell integrated UPQC (FCI-UPQC) is the combination of series and shunt connected active power filters with a fuel cell. The series active power filter [9] is used for voltage regulation [10] and voltage harmonic compensation and shunt active filter [11] is used to absorb current harmonics and compensate negative sequence currents.

The compensation by shunt active filter depends on reference current signal generated by the controller. The series active filter compensation depends on reference voltage signal generated by the controller. In recent years, several control techniques are used to generate reference signals for UPQC. However, artificial intelligence [12] based controller having higher impacts when compared with conventional controllers.

First, artificial neural networks (ANNs) are the electronic model based on the brain's neural structure. It is an interconnection of artificial neurons that can learn from experience to provide a decision that is more accurate. It has the ability to develop complex non-linear models with high speed and adaptability that can be trained at new frequencies [12]. Second, fuzzy logic is the technique which mimics the human reasoning capabilities and it consists of fuzzification, inference mechanism and defuzzification [13]. Khodayar *et al.* [14] have proposed a deep learning-based fuzzy inference model that can extract useful patterns from the input vectors to obtain more accurate fuzzy rules. Finally, the adaptive neuro-fuzzy inference system (ANFIS) combines both neural and fuzzy capabilities [15]. Here a neural network is used to automatically adjust membership functions and decrease the rate of errors to determine rules of the fuzzy logic. Usually, ANFIS [16] system prefers hybrid-learning algorithm for better ability, accelerate convergence and avoid the occurrence of a trapper in local minima. Hence, an adaptive network with back propagation algorithm is used in the ANN. The work in [17], evaluates a type-2 ANFIS that is more robust than the traditional ANFIS due to using interval knowledge. Also, Qureshi *et al.* [18] have proposed a recurrent neuro-fuzzy controller for fuel cell systems that bring more accuracy compared to the traditional feedforward one. In this paper, the synchronous reference frame (SRF) theory and instantaneous reactive power (IRP) theory are used to generate a reference voltage and reference current signals, respectively. The ANFIS controller with multi-layer feedforward neural network architecture is used for DC voltage regulation.

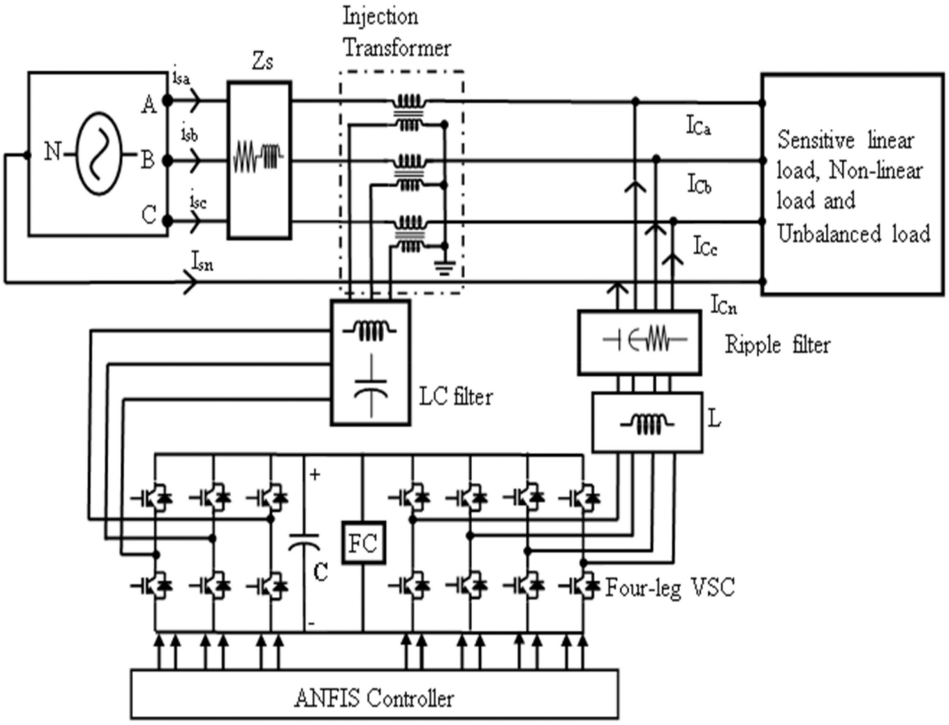

Fig. 1 *FCI-UPQC system configuration*

In recent years, renewable energy supported custom power devices are more attractive. In this work, the fuel cell-based UPQC is used to enhance the quality of power. The fuel cell is an electrochemical device that alters electrical power into chemical energy. Out of many fuel cells, available proton exchange membrane fuel cell (PEMFC) is most suitable for a distributed generation [19, 20]. Hence, PEMFC is preferred for this work. The two major roles of the proposed FCI-UPQC are to compensate the voltage fluctuations by injecting the appropriate voltage and to inject both reactive and harmonic components of load current to make source current as sinusoidal and balanced.

Besides the aforementioned technologies, the most important contribution of this work can be recapitulated as follows:

i. Analysis of Intelligent controller-based FCI-UPQC under voltage sag/swell on the source side and current harmonics on the load side.
ii. Performance investigation of the proposed system in the presence of source side voltage harmonics and current harmonics disturbances.
iii. Performance investigation of the proposed system in the presence of an unbalanced non-linear load.

2 Configuration of the proposed system

The proposed system consists of an FCI-UPQC with ANFIS controller. The topology of the proposed system is exposed in Fig. 1. It has two IGBT-based voltage source converter connected back-to-back through a common DC-link capacitor. The FC is integrated through DC-link of the UPQC. The shunt part of the FCI-UPQC has four-leg converter will inject both reactive and harmonic components of load current to make source current as sinusoidal and balanced. It also eliminates the neutral current through fourth-leg. Similarly, the series part of the FCI-UPQC having three-leg VSC and it will inject both fundamental and harmonic voltages. The series VSC is connected before sensitive linear load to protect the load from any voltage distortion from the source side and to make load voltage as sinusoidal.

The performance of the proposed system is analysed in the three-phase four-wire system with three different loads: non-linear, unbalanced, sensitive. Three-phase uncontrolled rectifier with resistive and inductive loads on the DC side acts as a non-linear load whereas three single-phase resistive and inductive loads with different rating act as an unbalanced load. Three-phase resistive and inductive loads are used as a sensitive linear load. These three loads are applied to different feeders.

The fuel cell is the energy conversion device, which generates electrical energy from the chemical energy. The fuel cell consists of two electrodes namely, anode and cathode. The electrolyte is filled between these two electrodes. The role of the electrolyte is to permit only Hydrogen ions to pass between electrodes and act as an insulator of electrons. Therefore, the electrons cannot pass through the membrane. Hence, the electron passes through the electrical circuit and generates an electrical current. Hydrogen atoms entering the fuel cell at the cathode lose its electrons due to the oxidation reaction. Simultaneously, oxygen atoms enter the fuel cell on the cathode side, there combines with electrons and produce harmless byproduct water. Multiple fuel cells are united to form a fuel cell stack. This fuel cell stack is used for island operation and real power support. A PEMFC consists of anode, cathode and a solid electrolyte between the two electrodes. A platinum catalyst is used to activate the reaction to obtain protons and electrons from hydrogen molecules. The produced electrons at the anode are given to the DC load and the protons go to the cathode through the exchange membrane. The oxygen near the cathode mingles with protons from the anode and electrons from the DC load to produce water [19, 20]. In this way, electricity is produced from the fuel cell as electrons flow from the anode to cathode through the DC load of the proposed system. The reactions near the anode, cathode and the overall chemical reaction of the fuel cell are given below [3, 21]:

$$H_2 = 2H^+ + 2e^- \tag{1}$$

$$\frac{1}{2}O_2 + 2H^+ + 2e^- = H_2O \tag{2}$$

$$H_2 + \frac{1}{2}O_2 = H_2O \tag{3}$$

A PEMFC stack is modelled upon considering the starting loss, absorption loss and ohmic losses. The anode pressure, cathode pressure, fuel cell initial temperature and room temperature are the inputs and the fuel cell voltage (V_{FC}) is the output of the proposed PEMFC model. Considering the double layer charging effect, the output voltage of the fuel cell V_{FC} can be obtained using the following equation:

$$V_{FC} = E - V_{a1} - V_{c1} - V_o \quad (4)$$

where E is the reversible potential, V_{a1} is the starting voltage fall, which is effected by the internal temperature of the fuel cell (T), V_{c1} is the concentration voltage drop and V_o is the ohmic voltage drop. The reversible potential E is calculated using Nernst (5)

$$E = E_0 + \frac{RT}{2F}\ln\left(p_{H_2} \times \sqrt{p_{O_2}}\right) \quad (5)$$

$$E_0 = E_0^o - k_E(T - 298) \quad (6)$$

where E_0 is the reference potential which is a function T, R is gas constant, 8.3143J/(mole, K), F is the Faraday constant, 96,487 (C/mole), $E_0{}^o$ is the standard reference potential at standard state, 298 K at 1 atm pressure, K_E is the empirical constant terms, p_{H_2} and p_{O_2} are the partial pressures of hydrogen and oxygen, respectively.

The empirical formulae for activation losses V_a are given below:

$$V_{a1} = \eta + a(T - 298) \quad (7)$$

$$V_{a2} = T \times b\ln(I_{FC}) \quad (8)$$

$$V_a = V_{a1} + V_{a2} = [(\eta + a(T - 298)) + (T \times b\ln(I_{FC}))] \quad (9)$$

where a, b are the empirical constant terms, η is the temperature invariant part of V_a in volts, T is the internal temperature, I_{FC} is the current from the fuel cell which determines T.

The absorption voltage drop is given below:

$$V_c = -\frac{RT}{zF}\ln\left(1 - \frac{I_{FC}}{I_{lim}}\right) \quad (10)$$

where I_{lim} is the limitation current (A), Z is the number of electrons

$$V_{c1} = \left(I_{FC} - C\frac{dV_2}{dt}\right)(R_a + R_c) \quad (11)$$

R_a and R_c are equivalent resistances of activation and concentration voltage drops. The equivalent resistance of activation (R_a) corresponding to V_{a2} is calculated by using the following equation:

$$R_a = \frac{V_{a2}}{I_{FC}} \quad (12)$$

The concentration equivalent resistance (R_c) is calculated by using the following equation:

$$R_c = \frac{V_c}{I_{FC}} \quad (13)$$

The ohmic voltage drop is calculated by

$$V_o = I_{FC}R_o \quad (14)$$

where R_o is the ohmic resistance

$$R_o = R_{o1} + k_{RI}I_{FC} + k_{RT}T \quad (15)$$

where R_{o1} is the constant part of R, k_{RI} is the empirical constant for calculating R_o, (r/A), k_{RT} is the empirical constant for calculating R_o, (r/K) content.

3 Control strategy

The DC-link derives reference signals. The difference between actual and reference signals is given to the controller. The output of the controller is given to the generation of pulses. In this paper, the ANFIS controller is used to extorting reference signals. The signal from this controller is extracted by shunt active filter using IRP algorithm. This reference current signal generated by ANFIS controller-based IRP theory is the main lead in providing compensation. Shunt active filter eliminates current harmonics, neutral current compensation, load balancing, power factor correction, voltage regulation in distributed systems and series active filter protects load voltage from any short duration voltage disturbances such as voltage sag, voltage swell and so on from the supply side and helps in harmonic reduction as well as active power injection to grid.

The ANFIS controller controls a small amount of active current by comparing with an actual DC-link voltage of shunt active filter with a reference voltage and the opposite of this control corresponds to power flow needed to maintain DC-link voltage. Hence, this power flow is added as part of reference for the current controller, which controls the inverter to provide the required compensation current and maintain the DC-link voltage of shunt active filter. In a similar manner, the reference voltage signal is used in the series active filter.

The proposed system uses the IRP theory together with a proportional–integral (PI) controller for both shunt and series components. The primary role of the series active filter is to compensate for voltage flaw by injecting appropriate voltage [22]. The voltage injected by the series active filter is in series with sensitive load through an injection transformer and LC filter, which are used to prevent, switching harmonics produced by VSC [23]. The DC voltage is connected to the DC side of VSC through a capacitor with fuel cells.

The data obtained from the PI controller is used as a training and checking data for ANFIS controller. This ANFIS controller provides compensation and balance in case of voltage sag, swell, harmonics, neutral current, source current balance and maintains the DC-link voltage.

3.1 Extraction of reference current using IRP theory

The ANFIS controller supported current reference signals control circuit is exposed in Fig. 2. The three-phase source voltages (V_{sa}, V_{sb}, V_{sc}) are converted to $V_{\alpha,\beta}$ coordinates by Clarke transformation using the following equations:

$$V_\alpha = \sqrt{\frac{2}{3}}\left[V_{sa} - \frac{V_{sb}}{2} - \frac{V_{sc}}{2}\right] \quad (16)$$

$$V_\beta = \left[\frac{V_{sb} - V_{sc}}{\sqrt{2}}\right] \quad (17)$$

Similarly, the three-phase load currents (I_{La}, I_{Lb}, I_{Lc}) are sensed and converted to $I_{0\alpha\beta}$ coordinates using the following equations:

$$I_0 = \sqrt{\frac{1}{3}}[I_{La} + I_{Lb} + I_{Lc}] \quad (18)$$

$$I_\alpha = \sqrt{\frac{2}{3}}\left[I_{La} - \frac{I_{Lb}}{2} - \frac{I_{Lc}}{2}\right] \quad (19)$$

$$I_\beta = \left[\frac{I_{La} - I_{Lc}}{\sqrt{2}}\right] \quad (20)$$

The instantaneous active power (P) and reactive power (Q) are calculated using formulae (21) and (22). The obtained real power P is partitioned into average real power and oscillating real power

$$P = V_\alpha I_\alpha + V_\beta I_\beta \quad (21)$$

$$Q = V_\beta I_\alpha - V_\alpha I_\beta \quad (22)$$

The harmonic active and reactive powers, which are obtained from P, are compensated using a low-pass filter. The output P_1 is summated with P_L to give P^*, the power flow needed to maintain

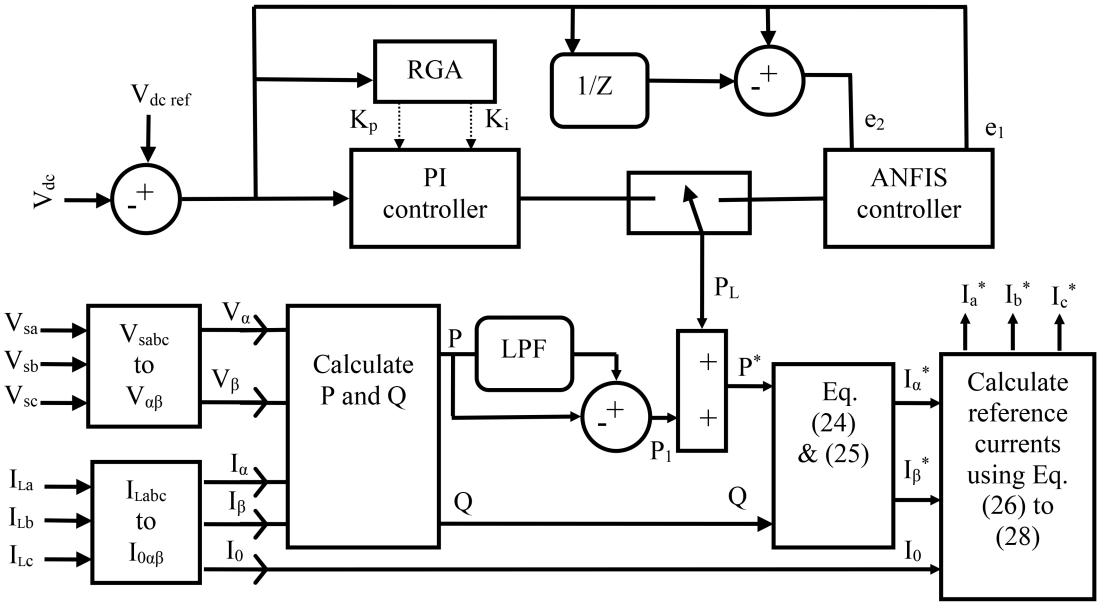

Fig. 2 *Extraction of reference current using ANFIS controller based IRP theory*

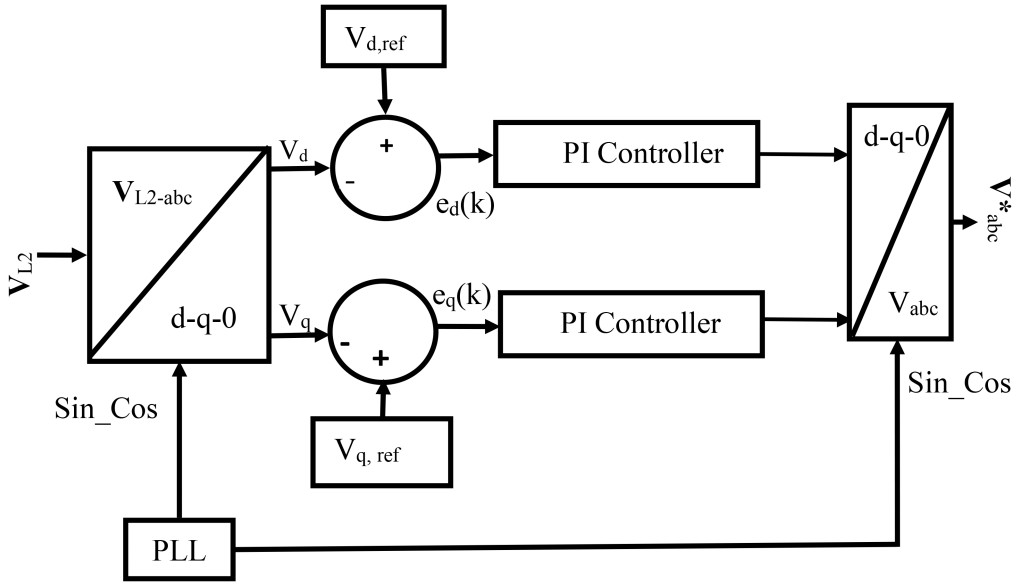

Fig. 3 *Extraction of the voltage reference for the series active filter*

DC-link voltage. P_L is obtained when the error between actual DC-link voltage and reference DC voltage is processed through a PI controller.

$$P^* = P_1 + P_L \tag{23}$$

$$I_\alpha^* = \left[\left(\frac{-1}{V_\alpha^2 + V_\beta^2}\right)((P^* \times V_\alpha) + (Q \times V_\beta))\right] \tag{24}$$

$$I_\beta^* = \left[\left(\frac{-1}{V_\alpha^2 + V_\beta^2}\right)((P^* \times V_\beta) - (Q \times V_\alpha))\right] \tag{25}$$

The voltage reference signals control circuit is exposed in Fig. 3. We calculate the $\alpha - \beta$ currents from P^* and Q which together with zero sequence current are converted to reference currents by using inverse Clarke transformation as exposed in the following equations:

$$I_a^* = \sqrt{\frac{2}{3}}\left[I_\alpha^* + \frac{I_0}{\sqrt{2}}\right] \tag{26}$$

$$I_b^* = \sqrt{\frac{2}{3}}\left[\frac{-I_\alpha^*}{2} + \frac{\sqrt{3}}{2}I_\beta^* + \frac{I_0}{\sqrt{2}}\right] \tag{27}$$

$$I_c^* = \sqrt{\frac{2}{3}}\left[\frac{-I_\alpha^*}{2} - \frac{\sqrt{3}}{2}I_\beta^* + \frac{I_0}{\sqrt{2}}\right] \tag{28}$$

Error signals were produced when the generated reference currents I_a*, I_b* and I_c* are compared with the source currents I_{sa}, I_{sb} and I_{sc} and fed to the controller to generate the firing pulses for the IGBT switches.

3.2 Extraction of reference voltage using SRF theory

Using the park transformation, the three-phase voltage across the sensitive load is sensed and converted into *d–q–o* components as exposed in (29)–(31) to separate zero sequence component from the *abc* phases so that the *d–q* components can be easily controlled [3]

$$V_d = \frac{2}{3}[V_{L2a}\sin\omega t + V_{L2b}\sin(\omega t - 2\pi/3) + V_{L2c}\sin(\omega t + 2\pi/3)] \tag{29}$$

$$V_q = \frac{2}{3}[V_{L2a}\cos\omega t + V_{L2b}\cos(\omega t - 2\pi/3) + V_{L2c}\cos(\omega t + 2\pi/3)] \tag{30}$$

$$V_O = \frac{1}{3}[V_{L2a} + V_{L2b} + V_{L2c}] \tag{31}$$

where V_{L2a}, V_{L2b} and V_{L2c} have sensed load voltages across the sensitive load. In order to detect the phase and change in load voltage, the d–q components along with unit vectors ($\sin\theta$, $\cos\theta$) are derived from the phase locked loop (PLL). The rated voltage 1 pu is set as a reference for d-component ($V_{d,\,\mathrm{ref}}$) and zero pu is set as a reference for q-component ($V_{q,\mathrm{ref}}$). The error between the actual voltage and the reference voltage in the d–q frame is used to detect voltage sag and swell [3].

This error is processed through an individual PI controller for d-component and q-component. Using inverse park transformation, the reference voltage signal is generated by the output from the controller. Using (32)–(34), the d–q components are converted into abc phases in the absence of sequence component (V_o).

$$V_a^* = V_d\sin\omega t + V_q\cos\omega t \tag{32}$$

$$V_b^* = V_d\sin(\omega t - 2\pi/3) + V_q\cos(\omega t - 2\pi/3) \tag{33}$$

$$V_c^* = V_d\sin(\omega t + 2\pi/3) + V_q\cos(\omega t + 2\pi/3) \tag{34}$$

These abc components are given to the VSC through the PWM pulse generator. Hence, the FCI-UPQC is fully capable to inject or absorb the required voltage whenever the voltage sag and swell are detected from the sensitive load voltage. The optimised values of K_p and K_i of the PI controller of the DSTATCOM are 4.96 and 1.01, respectively [9]. Equation (35) obtains the reference current signal for fourth-leg of VSC in FCI-UPQC

$$i_n^* = -(i_{La} + i_{Lb} + i_{Lc}) \tag{35}$$

By comparing the actual load current with the reference value, an error signal is produced which is used to generate switching signals for the fourth-leg of VSC in FCI-UPQC. The reference for neutral current is set at zero. The generated reference current signal is fed to the controller to generate switching pulses for IGBT switches.

3.3 DC voltage regulation using ANFIS controller

The difference between actual DC-link voltage and the reference voltage are given to the ANFIS controller. The output of the controller is used to generate pulses to control the IGBTs of the converter. The real number genetic algorithm was successfully used to optimise the PI controller parameters [24]. The non-linearity of loads leads to distortions in the signals that are usually rectified by using traditional PI controllers that can fail in providing high accuracy, fast processing of the reference signal. Hence, ANFIS controller with the high dynamic response is used for maintaining the stability of the converter system over the wide operating range. The ANFIS controller combines both the learning abilities of a neural network and reasoning abilities of fuzzy logic. The ANFIS controller uses the hybrid algorithm, a combination of the least-squares method and back propagation gradient descent method. The ANFIS is given with two inputs e_1 and e_2, where the error between actual and reference DC voltages is e_1 and change in error as e_2.

There are five layers of ANFIS architecture. In Fig. 4, all the square nodes are adaptive, their parameters can be changed during training, and all the nodes in the circle have fixed parameters. Layers 1 and 4 are adaptive nodes and remaining are circle nodes. Parameters of layer-1 are called premise parameters and that of layer-4 are consequent parameters. The least-squares method is used in a forward pass by fixing the premise parameters and adjusting consequent. The gradient descent method is used in a backward pass in which error signals propagate backward by

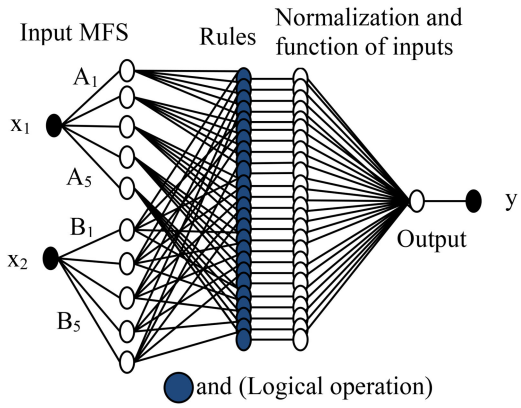

Fig. 4 *ANFIS architecture*

adjusting premise parameters and fixing the consequent parameters.

Layer 1: e_1 is the input to node 1, A_i is the linguistic label linked with this node function, and seven triangular membership functions are used. The node equation is given below:

$$O_i^1 = \mu A_i(e_1), \quad \mu B_i(e_2) \tag{36}$$

$$\mu A_i(e_1), \quad \mu B_i(e_2) = \begin{cases} 0 & e_1 \le a_i \\ \dfrac{e_1 - a_i}{b_i - a_i} & a_i \le e_1 \le b_i \\ \dfrac{c_i - e_1}{c_i - b_i} & b_i \le e_1 \le c_i \\ 0 & c_i \le e_1 \end{cases} \tag{37}$$

where $i = 1, 2, \ldots, 7$. O_i^1 is the output of the ith node in layer 1, a_i, b_i, c_i are the parameters of the triangular membership functions.

Layer 2: The node is labelled as $\prod$. The incoming signals from layer 1 are multiplied and sent to layer 3

$$\omega_j = \mu A_i(e_1) \times \mu B_i(e_2) \tag{38}$$

where $i = 1, 2, \ldots, 7$ and $j = 1, 2, 3, \ldots, 49$.

The firing strength of a rule is represented by the nodal output.

Layer 3: It is labelled as n. The normalised firing strength of every rule is calculated using the output of this layer

$$\overline{\omega_j}\frac{\omega_j}{\sum_{k=1}^{49}\omega_k} \tag{39}$$

where $j = 1, 2, \ldots, 7$.

Layer 4: The parameters of this layer are called consequent parameters

$$O_j^4 = \overline{\omega_j} f_j = \overline{\omega_j}(r_j e_1 + s_j e_2 + t_j) \tag{40}$$

Rules

If $e_1 = A_1$ and $e_2 = B_1$ then $f_1 = r_1 \cdot e_1 + s_1 \cdot e_2 + t_1$

If $e_1 = A_1$ and $e_2 = B_2$ then $f_2 = r_2 \cdot e_1 + s_2 \cdot e_2 + t_2$

$\vdots$

If $e_1 = A_7$ and $e_2 = B_7$ then $f_{49} = r_{49} \cdot e_1 + s_{49} \cdot e_2 + t_{49}$

where O_j^4 is the output of the ith node in layer 4, $\overline{\omega_j}$ is the output from layer 3, r_j, s_j, t_j are the consequent parameters set which are determined during training, A_i, B_i are the fuzzy membership functions, $i = 1, 2, \ldots, 7$ and $j = 1, 2, 3, \ldots, 49$.

Layer 5: This layer is the summation of all the incoming signals and is given as y

$$y = \sum_{j=1}^{49} \overline{\omega_j} f_j = \sum_{j=1}^{49} \left[(\overline{\omega_j} e_1) r_j + (\overline{\omega_j} e_2) s_j + (\overline{\omega_j}) t_j \right] \quad (41)$$

The results illustrate the evident impact of e_1 on voltage regulation. The ANFIS in the proposal uses 49 rules with seven membership functions for each input variable. The ANFIS used was trained with 60,001 data and the data verified was checked with 60,000 checking data. Comparing the actual DC-link voltage and reference, the ANFIS controller controls the small amount of active current. The DC link is maintained by the power flow developed corresponding to the output of the controller. The power flow is added as a reference for a current controller that controls the inverter to provide the required compensation current to maintain the voltage of FCI-UPQC.

4 Results and discussion

The performance of the proposed FCI-UPQC is analysed with linear, nonlinear and unbalanced loads under various situations with ANFIS controller using MATLAB/SIMULINK. All the voltage measurements are expressed in per unit system and the current measurement in the actual value system. In the proposed work, the shunt converter of FCI-UPQC is switched on at 0.05 s to clearly represent the role of the shunt converter.

The sub-plots of Fig. 5 illustrate the performance of FCI-UPQC with ANFIS controller under voltage sag and swell conditions, here the source voltage sag takes place during 0.5–1 s and a voltage swell from 0.15 to 0.2 s. During sag conditions, the corresponding injected voltage will be in phase with the source voltage and during voltage swell conditions the injected voltage will be 180° out of phase with the source voltage. Since the load is non-linear, the load current is not sinusoidal. Hence the authors are using FCI-UPQC to compensate and maintain the quality of source current waveform. During 0–0.05 s, the shunt converter is in off condition, so that the load current will be same as that of the source current without any compensation.

In the sub-plots of Fig. 6, the harmonic disturbances are introduced in source side voltage and current from 0.1 to 0.2 s under non-linear load conditions and its corresponding response (load voltage and source current) was obtained. It is observed that from 0.1 to 0.2 the source current harmonics cannot be eliminated by the FCI-UPQC.

Fig. 7 illustrates that the percentage THD in voltage is reduced largely after compensation. The main aim of converter current (I_C) is to maintain source current (I_S) as sinusoidal, balanced and in phase with source voltage (V_S). Hence, it provides the required compensation to load current (I_L) whenever there is an unbalance. Since the load is unbalanced, the load current is not in phase with the source voltage. Hence the authors are using FCI-UPQC to compensate and maintain I_S.

Fig. 8 illustrates that the percentage total harmonic distortion (THD) in current is being reduced mostly after compensation. It is

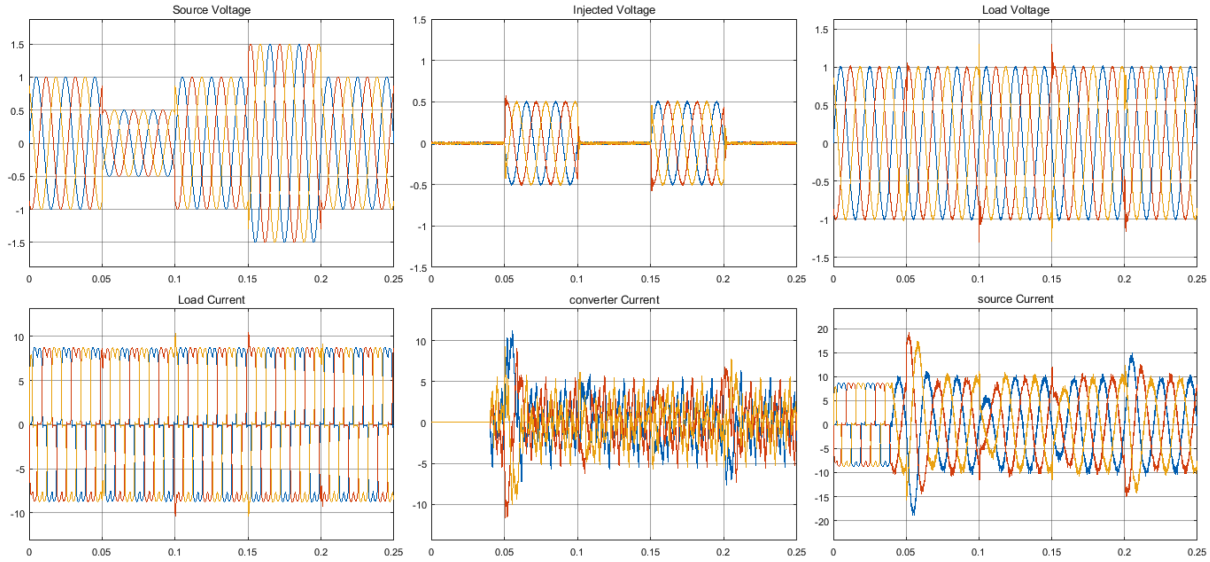

Fig. 5 *Performance of FCI-UPQC under voltage sag, swell and current harmonics disturbances*

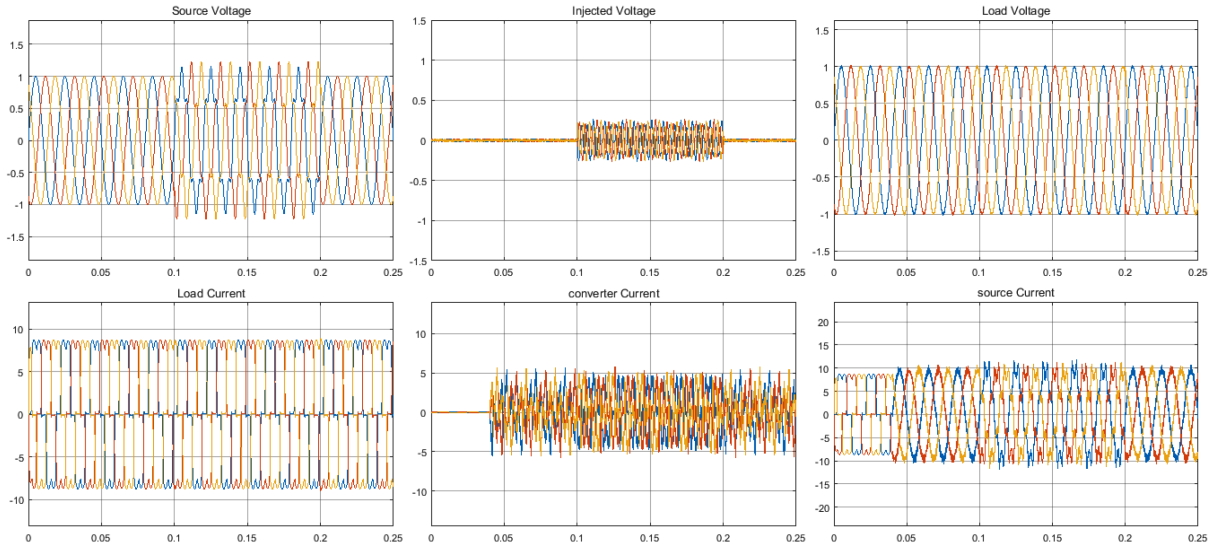

Fig. 6 *Performance of FCI-UPQC under source side voltage and current harmonics disturbances*

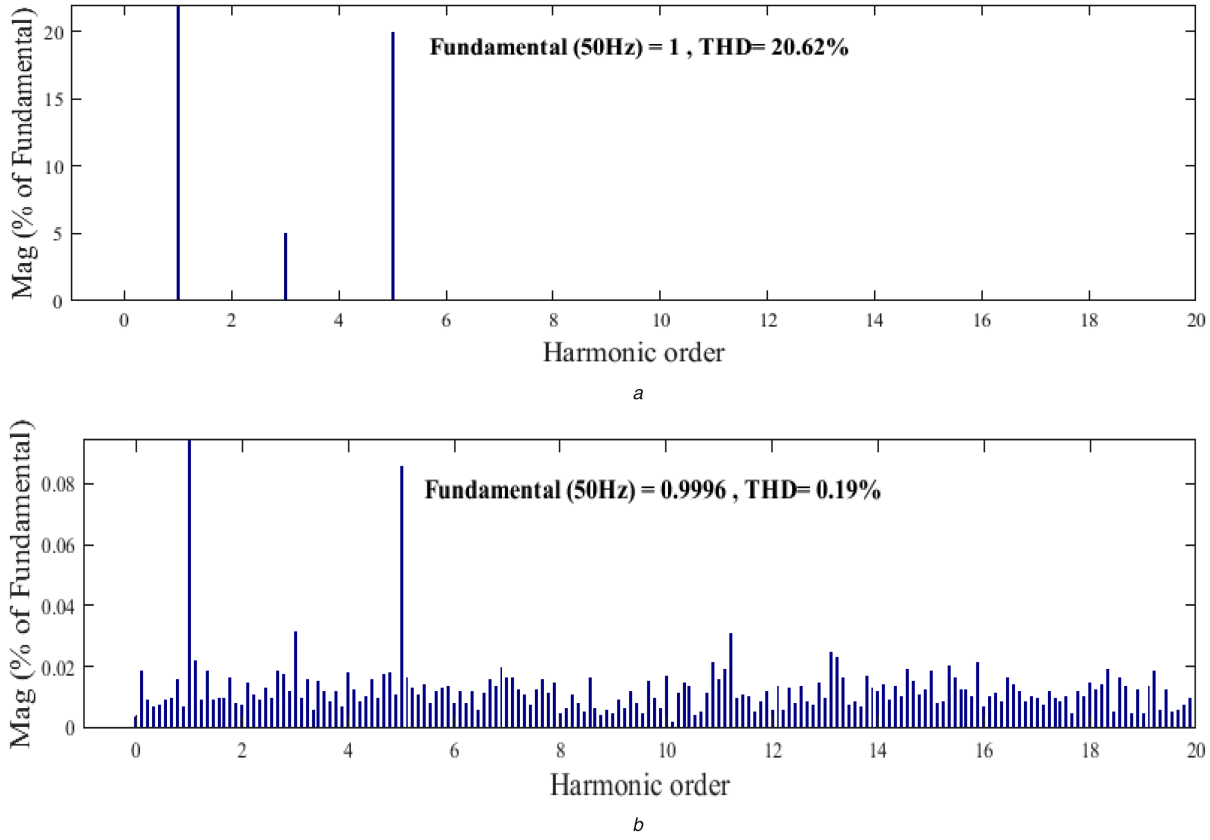

Fig. 7 *Voltage THD compensation*
(a) Before compensation, ***(b)*** After compensation

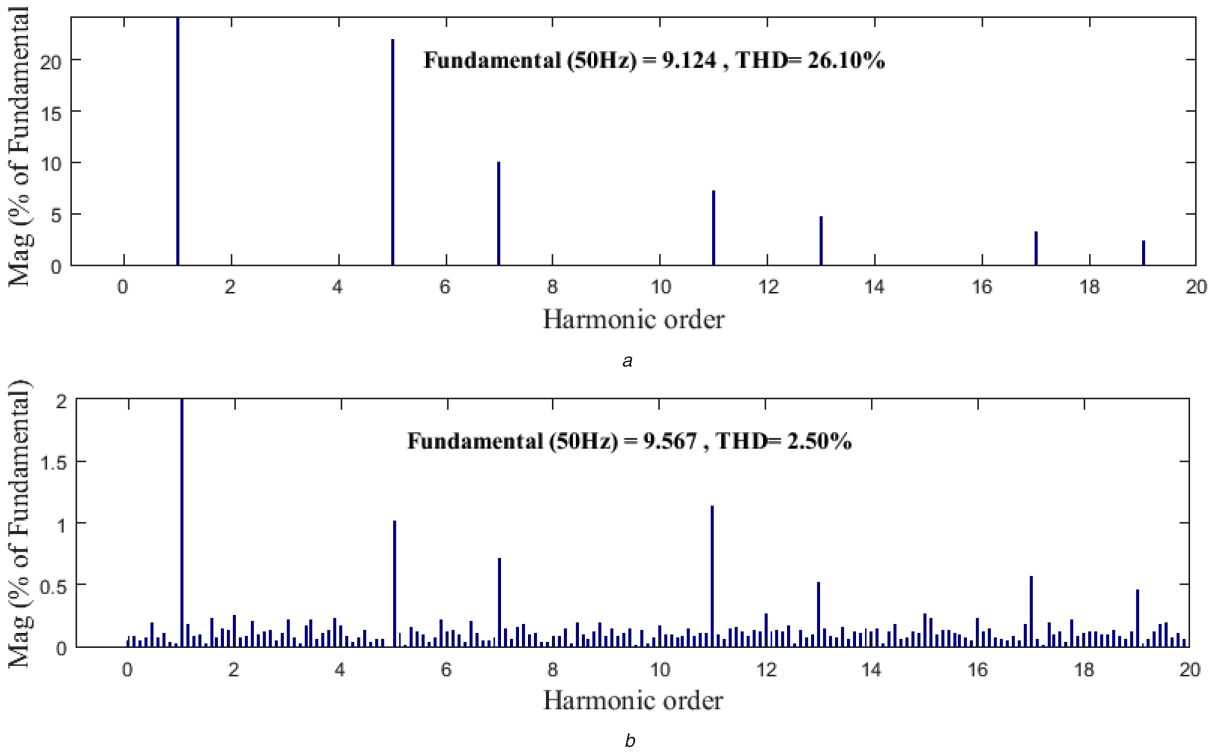

Fig. 8 *Current THD compensation*
(a) Before compensation, ***(b)*** After compensation

evident that THD of source current decreases with the help of the ANFIS controller and fulfil the requirement of the IEEE-519 standard.

The individual harmonic spectrum of source current before and after compensation with ANFIS controller is exposed in Table 1. It is observed that all the individual harmonics are reduced by the proposed system.

Table 2 illustrates the voltage and current THD comparison between the proposed method and the literature results. It is observed that the proposed method is more efficient than conventional methods.

Consider a situation described in Fig. 9 under unbalanced load condition, let us say that the b-phase current is suppressed during 0.1 to 0.2 s, and then there will be a respective converter current

Table 1 Harmonic spectrum of source current after compensation with ANFIS controller

Harmonics number	Before compensation, %	After compensation, %
3	0.02	0.22
5	22.06	1.02
7	10.12	0.71
9	0.02	0.09
11	7.28	1.14
13	4.79	0.52
15	0.01	0.27
17	3.25	0.57
19	2.40	0.46
THD	26.10	2.50

Table 2 Comparison of harmonic compensation with different controllers

Voltage/current	THD (%) in sensitive load voltage and source current		
	Kinhal *et al.* [12]		Proposed method
	PI controller, %	ANN controller, %	ANFIS controller, %
load voltage	20.7	25.5	0.19
source current	8.4	8.8	2.50

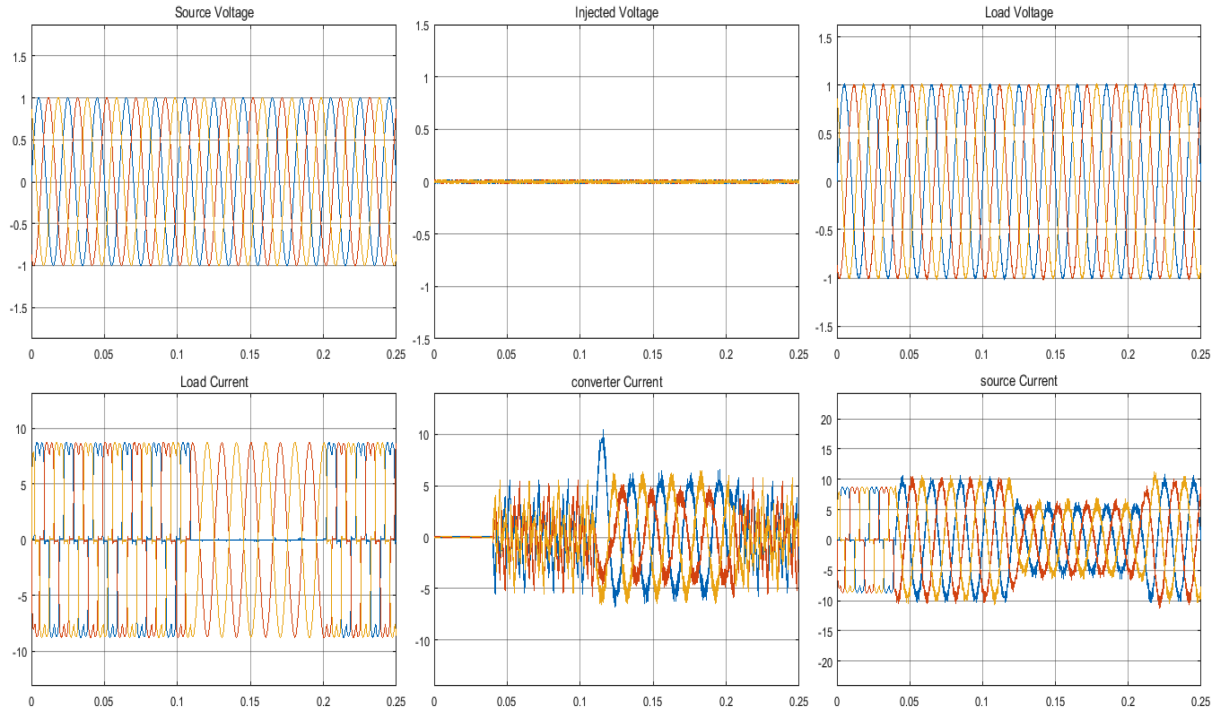

Fig. 9 *Performance of FCI-UPQC under current harmonics with the unbalanced load conditions*

addition to maintain the source current waveform quality. In addition, the load neutral current (I_n) produced during the unbalanced load need to be cancelled hence a converter neutral current I_{cn} is injected in opposite phase to maintain the source side neutral current almost near to zero. ANFIS controller offers better harmonic compensation in the distribution grid.

5 Conclusion

In this paper, a novel utility of FCI-UPQC as a compensating and an interconnecting device for a three-phase four-wire distribution grid is extensively simulated in MATLAB/SIMULINK. It was observed that the proposed FCI-UPQC efficiently compensates the problem of load current and supply voltage imperfections with quick response and high reliability at the same time. The proposed system has an enhanced performance under unbalanced, non-linear and sensitive linear load conditions. It is important to note that the proposed system still having the challenge to mitigate source current harmonics during source side disturbances and the type-2 ANFIS controlled FCI-UPQC is another scope for the future work.

6 Acknowledgments

The authors gratefully acknowledge the management of SASTRA Deemed to be University, Thanjavur, India, for providing all facilities to do the research work.

7 References

[1] Naderi, Y., Hosseini, S.H., Zadeh, S.G., *et al.*: 'An overview of power quality enhancement techniques applied to distributed generation in electrical distribution networks', *Renew. Sustain. Energy Rev.*, 2018, **93**, pp. 201–214

[2] Ghosh, A., Ledwich, G.: '*Power quality enhancement using custom power devices*' (Kluwer Academic Publishers, London, 2002)

[3] Sundarabalan, C.K., Selvi, K.: 'Real coded GA optimized fuzzy logic controlled PEMFC based dynamic voltage restorer for reparation of voltage disturbances in distribution system', *Int. J. Hydrog. Energy*, 2017, **42**, (1), pp. 603–613

[4] Khadkikar, V.: 'Enhancing electric power quality using UPQC: A comprehensive overview', *IEEE Trans. Power Electron.*, 2012, **22**, (7), pp. 2284–2297
[5] Jayanti, N.G., Basu, M., Conlon, M.F., *et al.*: 'Rating requirements of the unified power quality conditioner to integrate the fixed-speed induction generator-type wind generation to the grid', *IET Renew. Power Gener.*, 2009, **3**, (2), pp. 133–143
[6] Palanisamy, K., Kothari, D.P., Mahesh, K.M., *et al.*: 'Effective utilization of unified power quality conditioner for interconnecting PV modules with grid using power angle control method', *Int. J. Electr. Power Energy Syst.*, 2013, **48**, pp. 131–138
[7] Ghosh, A., Ledwich, G.: 'A unified power quality conditioner (UPQC) for simultaneous voltage and current compensation', *Electr. Power Syst. Res.*, 2001, **59**, (1), pp. 55–63
[8] Monteiro, L.F.C., Aredes, M., Pinto, J.G., *et al.*: 'Control algorithms based on the active and non-active currents for a UPQC without series transformers', *IET Power Electron.*, 2016, **9**, (9), pp. 1985–1994
[9] Sundarabalan, C.K., Selvi, K.: 'Compensation of voltage disturbances using PEMFC supported dynamic voltage restorer', *Int. J. Electr. Power Energy Syst.*, 2015, **71**, pp. 77–92
[10] Tang, S., Tesler, F., Marlasca, F.G., *et al.*: 'Shock waves and commutation speed of memristors', *Phys. Rev. X*, 2016, **6**, (1), p. 011028
[11] Singh, B., Jayaprakash, P., Kothari, D.P.: 'New control approach for capacitor supported DSTATCOM in three-phase four wire distribution system under non-ideal supply voltage conditions based on synchronous reference frame theory', *Int. J. Electr. Power Energy Syst.*, 2011, **33**, pp. 1109–1117
[12] Kinhal, V.G., Agarwal, P., Gupt, H.O.: 'Performance investigation of neural-network-based unified power-quality conditioner', *IEEE Trans. Power Deliv.*, 2011, **26**, (1), pp. 431–437
[13] Berbaoui, B.: 'Fuzzy multi-objective technique combined with VCS algorithm for unified power quality conditioner based on hybrid power source PEMFC/SC', *Int. J. Hydrog. Energy*, 2018, **43**, pp. 6275–6293
[14] Khodayar, M., Wang, J., Manthouri, M.: 'Interval deep generative neural network for wind speed forecasting', *IEEE Trans. Smart Grid*, in press, doi: 10.1109/TSG.2018.2847223
[15] Jang, J.S.R.: 'ANFIS adaptive network based fuzzy interface system', *IEEE Trans. Syst. Man Cybern.*, 1993, **23**, pp. 665–684
[16] Lin, C.T., Lee, C.G., Lin, C.T., *et al.*: '*Neural fuzzy systems: a neuro-fuzzy synergism to intelligent systems*', vol. **205** (Prentice hall PTR, Upper Saddle River, NJ, 1996)
[17] MonirVaghefi, H., Rafiee Sandgani, M., Aliyari Shoorehdeli, M.: 'Interval type-2 adaptive network-based fuzzy inference system (ANFIS) with type-2 non-singleton fuzzification'. 2013 13th Iranian Conf. on Fuzzy Systems (IFSC), Qazvin, Iran, 2013
[18] Qureshi, M., Qamar, S., Ali, S., *et al.*: 'Recurrent neuro-fuzzy control of grid-interfaced solid oxide fuel cell system', *Int. J. Syst. Control Commun.*, 2018, **9**, (1), p. 31
[19] Hashem Nehrir, M., Wang, C.: '*Modeling and control of fuel cells distributed generation application*' (John Wiley & Sons Inc., Hoboken, 2009)
[20] Wee, J.H.: 'Applications of proton exchange membrane fuel cell systems', *Renew. Sustain. Energy Rev.*, 2007, **11**, (8), pp. 1720–1738
[21] Hatti, M., Meharrar, A., Tioursi, M.: 'Power management strategy in the alternative energy photovoltaic/PEM fuel cell hybrid system', *Renew. Sustain. Energy Rev.*, 2011, **15**, (9), pp. 5104–5110
[22] Jowder, F.A.L.: 'Design and analysis of dynamic voltage restorer for deep voltage sag and harmonic compensation', *IET Gener. Transm. Distrib.*, 2009, **3**, pp. 547–560
[23] Salimin, R.H., Rahim, M.S.A.: 'Simulation analysis of DVR performance for voltage sag mitigation'. IEEE Conf. on Power Engineering and Optimization (PEOCO), Shah Alam, Malaysia, 2011, pp. 261–266
[24] Sundarabalan, C.K., Selvi, K.: 'PEM fuel cell supported distribution static compensator for power quality enhancement in three-phase four-wire distribution system', *Int. J. Hydrog. Energy*, 2014, **39**, (33), pp. 19051–19066